

We are IntechOpen, the world's leading publisher of Open Access books Built by scientists, for scientists

6,900

Open access books available

185,000

International authors and editors

200M

Downloads

Our authors are among the

154

Countries delivered to

TOP 1%

most cited scientists

12.2%

Contributors from top 500 universities



WEB OF SCIENCE™

Selection of our books indexed in the Book Citation Index
in Web of Science™ Core Collection (BKCI)

Interested in publishing with us?
Contact book.department@intechopen.com

Numbers displayed above are based on latest data collected.
For more information visit www.intechopen.com



Micro-Solid-State Laser for Ignition of Automobile Engines

Masaki Tsunekane, Takayuki Inohara, Kenji Kanehara and Takunori Taira
Institute for Molecular Science, Nippon Soken, Inc.
Japan

1. Introduction

Recently in consideration of the problem of protecting the global environment and preserving fossil resources, the research and development of new clean vehicles driven by clean energy sources, such as electricity, fuel cell, etc., has been progressing worldwide. However it is difficult to replace all conventional gasoline vehicles to clean vehicles immediately, because they still have several hurdles to get over, costs of the clean vehicles and the energy sources, range between refuelling, the availability of refuelling or recharging stations, vehicle performance, fuel cell lifetime, etc. Therefore the improvement of the efficiency of conventional internal combustion gasoline engines, and the reductions of CO₂ and harmful pollutant emissions have become more important today.

A laser has been discussed widely as one of the promising alternatives for an ignition source of the next generation of efficient internal combustion engines (Hickling & Smith, 1974; Dale et al., 1997; Phuoc, 2006). Laser ignition can change the concept of ignition innovatively and has many advantages over conventional electric spark plug ignition. Figure 1 shows the schematics of combustion engines ignited by (a) an electric spark plug and a laser (b), (c).

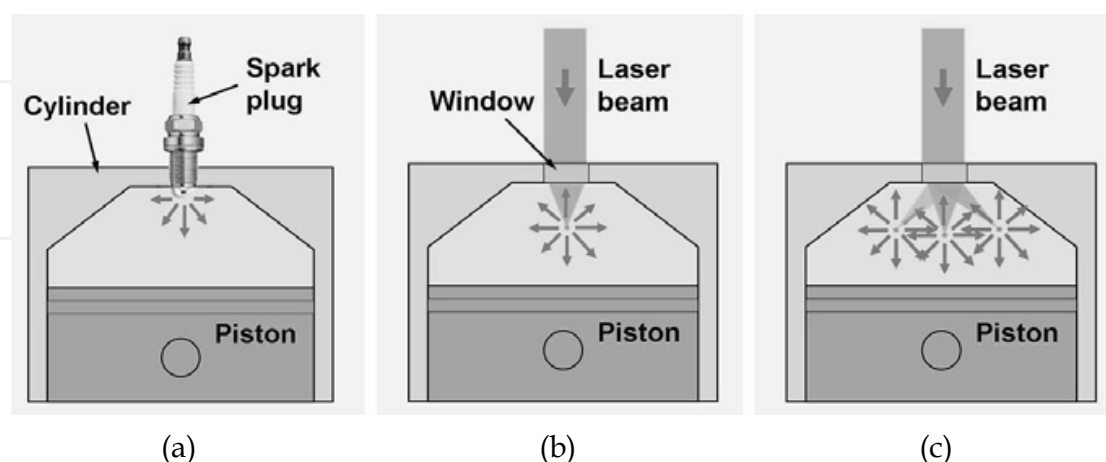


Fig. 1. Schematics of the combustion engines ignited by (a) a spark plug and (b), (c) a laser. (c) shows multipoint ignition.

Using a laser, the ignition plasma may be located anywhere within the combustion chamber because laser ignition doesn't need electrodes. Optimal positioning of ignition apart from

Source: Advances in Solid-State Lasers: Development and Applications, Book edited by: Mikhail Grishin, ISBN 978-953-7619-80-0, pp. 630, February 2010, INTECH, Croatia, downloaded from SCIYO.COM

the cold cylinder wall allows the combustion flame front to expand rapidly and uniformly in the chamber and thus increases the efficiency as seen in (b). In addition, laser ignition has great potential for simultaneous, spatial multipoint ignition within a chamber as shown in (c). This shortens combustion time dramatically and improves the output and efficiency of engines effectively (Phuoc, 2000; Morsy et al., 2001). Further a laser can ignite leaner or high-pressure mixtures that are difficult to be ignited by a conventional electric spark plug (Weinrotter et al., 2005). A laser igniter is also expected to have a longer lifetime than a spark plug due to the absence of electrodes.

One of the major difficulties of laser ignition for actual applications, especially for automobiles is the dimension of the lasers. For breakdown in fuel mixtures, light intensities in the order of $100\text{GW}/\text{cm}^2$ are necessary at the focal point of ignition. Then lasers with pulse energies higher than 10mJ , beam quality factors, M^2 of lower than 3 and pulse durations of shorter than 10ns have been used for combustion experiments. But the commercially available laser heads have table top size due to the complexities of the laser cavity and the cooling system.

In reductions of system size and costs, a multiplexing fiber optics delivery system seems to be ideal and practical for laser ignition of multicylinder engines. But it is difficult to deliver ignition light through fibers to each cylinder of an engine directly, because the optical damage threshold of fibers is still several orders of magnitude less than the peak energy levels required by laser ignition at present (Joshi et al., 2007). The fundamental problem of a fiber is attributed to the need to deliver relatively high power pulses with sufficient beam quality to focus the output light to the intensity required for breakdown.

2. Characteristics of passively Q-switched laser

A passively Q-switched solid-state laser, especially a Nd:YAG/Cr⁴⁺:YAG laser end-pumped by a fiber-coupled laser diode (LD) has been proposed as a promising ignition laser recently (Kofler et al., 2007). It has a simple structure, only two functional optical elements and no external power for optical switching is necessary hence the dimension of the laser head can be reduced. In addition, a short pulse operation less than 1ns is easily obtained by reduction of the cavity length less than 10mm and the beam quality is also good due to the soft aperture effect of a Cr:YAG saturable absorber (Zaykowski & Dill III, 1994; Sakai, 2008). The fiber delivered pump system allows not only further size reduction but also reliable laser operation, because the pump LD which is very sensitive to environmental temperature can be positioned at relatively stable place inside a car apart from the hot engine.

In generally, passively Q-switched lasers have large pulse-to-pulse energy fluctuations and large timing jitters under continuous-wave (CW) pumped operations (Huang et al., 1999; Tang et al., 2003) due to thermal and mechanical instabilities. Such fluctuations and jitters have strongly restricted the applications of passively Q-switched lasers. On the other hand, operation frequency of igniters of internal combustion engines is less than 60Hz , corresponding to an engine speed of 7200rpm , and the duty cycle is less than 5% for automobiles. In such a low frequency, quasi-continuous-wave (QCW) pumped operations with a low duty cycle, passively Q-switched lasers are expected to operate stably due to initialization of the thermal and mechanical conditions during pulses.

The characteristics of passively Q-switched lasers have been analyzed in detail and various optimum design criteria have been presented (Szabo & Stein, 1965; Degnan, 1995; Xiao & Bass, 1997; Zhang et al., 1997; Chen et al., 2001; Pavel, 2001; Patel & Beach, 2001). But there

are still several discrepancies in the theoretical calculations and the experimental results especially for output energy and efficiency. We think that the main cause is uncertainty of size of the laser mode. It is not easy to estimate the actual laser mode size and the beam quality accurately, because the aperture formed in the saturable absorber of a Cr:YAG crystal has a complex spatial distribution of transmission and it changes dynamically (Zabkar et al., 2008).

In this paper we demonstrated the optimum design of a high-brightness (high peak power and high beam quality), passively Q-switched micro-solid-state laser for ignition of engines. The performance of the micro-laser including fluctuations of pulse-to-pulse energy and timing jitters in QCW pumped operations was evaluated in detail. The combustion experiments in a static test chamber and a dynamic real automobile engine ignited by the micro-laser were demonstrated and discussed compared to a conventional spark plug. From the results, we could confirm that a high-brightness laser could dramatically reduce the minimum ignition energy and we also found that multi-pulse (pulse-train) ignition was effective to improve ignition possibility for leaner mixtures. Finally we successfully demonstrated the prototype laser igniter which had the same dimension as a spark plug including all optics for ignition.

3. Performance of micro-solid-state laser for ignition

3.1 Performance of passively Q-switched micro-laser module

Figure 2 shows (a) a schematic drawing and (b) a photograph of a passively Q-switched micro-laser module (Tsunekane et al., 2008). An active medium of a 1.1at.% Nd doped YAG crystal (crystal orientation of $\langle 111 \rangle$, Sumitomo Metal Mining Co., Ltd.) with a length of 4mm is longitudinally pumped by a fiber-coupled, conductive-cooled, 120W (peak) QCW 808nm laser diode (JENOPTIK laserdiode GmbH). The core diameter of the fiber is 0.6mm with N.A. of 0.22. The pump light from the fiber was collimated by a lens set to have a diameter of 1.1mm in the active medium. Antireflection ($<0.2\%$) and high-reflection ($>99.8\%$) coatings at 808nm and 1064nm, respectively, were deposited on the pumped surface of the Nd:YAG crystal. High-reflection ($>90\%$) and antireflection ($<0.2\%$) coatings at 808nm and 1064nm, respectively, were deposited on the other, intra-cavity surface of the

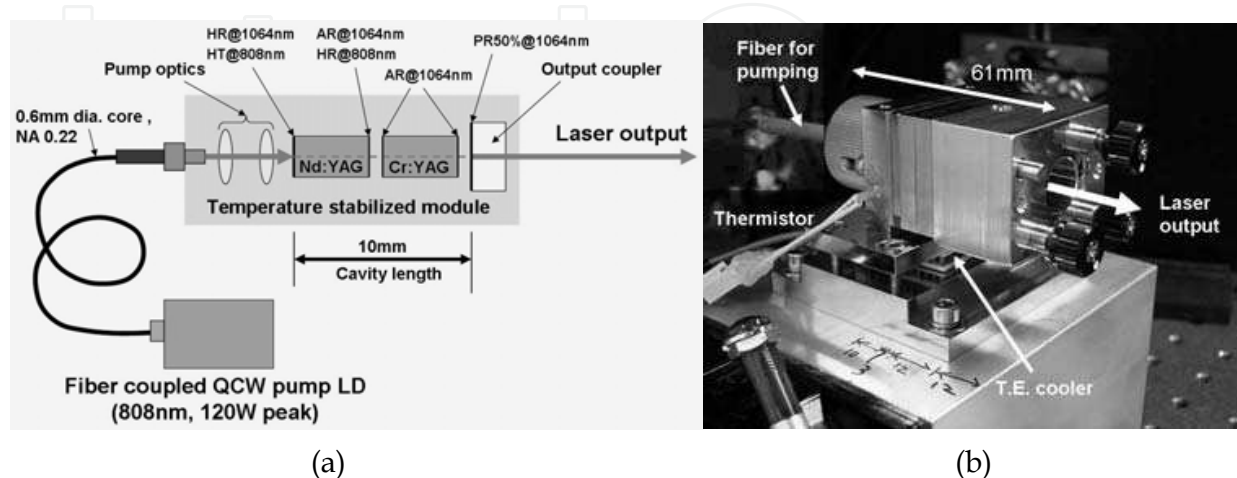


Fig. 2. (a) Schematic drawing and (b) photograph of the passively Q-switched micro-laser module.

crystal. The high-reflection coating at 808nm makes efficient pump absorption possible by a round trip path of the pump light and it can also prevent a closely situated Cr:YAG crystal from pump-induced breaching (Zaykowski & Wilson, Jr., 2003; Jaspan et al., 2004). Antireflection (<0.2%) coatings at 1064nm were deposited on both surfaces of the saturable absorber of a Cr⁴⁺:YAG crystal with a length of ~4mm (crystal orientation of <100>, Scientific Materials Corp.). The output coupler is flat with a reflectivity of 50% at 1064nm. The cavity length is 10mm. These optical elements were aligned carefully with an output coupler and fixed in the conductive-cooled, temperature-stabilized module (40mm-width × 28mm-height × 61mm-length) as shown in the figure. The module does not include focusing optics of the output beam for breakdown. In the following experiments, the pump energy was controlled by changing the pump duration with the peak pump power maintained at 120W. The maximum pump duration is 500μs limited by the diode. The repetition rate was 10Hz constant.

Figure 3 (a) shows the output energy of the passively Q-switched micro-laser as a function of the initial transmission of a Cr:YAG crystal. The output of a passively Q-switched laser forms a pulse train, which is well known. The closed circles and the solid line denote the experimental values and the calculation of pulse energy (energy per pulse), respectively, and the open circles denote the experimental values of the total output energy (sum of pulse energies) at a pump duration of 500μs. The pulse energy increases to 4.3mJ as an initial transmission of the Cr:YAG crystal decreases to 15%. On the other hand, the total output energy decreases from 25 to 12mJ as an initial transmission decreases from 80% to 15%, because the pulse-to-pulse interval becomes longer and then the number of laser pulses decreases even though the pulse energy increases. The decrease in total output energy simply means the decrease in efficiency of the laser.

Figure 3 (b) shows the pulse width as a function of the initial transmission of a Cr:YAG crystal. The pulse width was measured by a 10GHz InGaAs detector (ET-3500, Electro-Optics Technology, Inc.) with a 12GHz oscilloscope (DSO81204B, Agilent Technology). The closed circles and broken line denote the experimental values and the calculation of the pulse width, respectively. The pulse width decreases as the initial transmission decreases. The shortest pulse width of 300ps was obtained at an initial transmission of 15%.

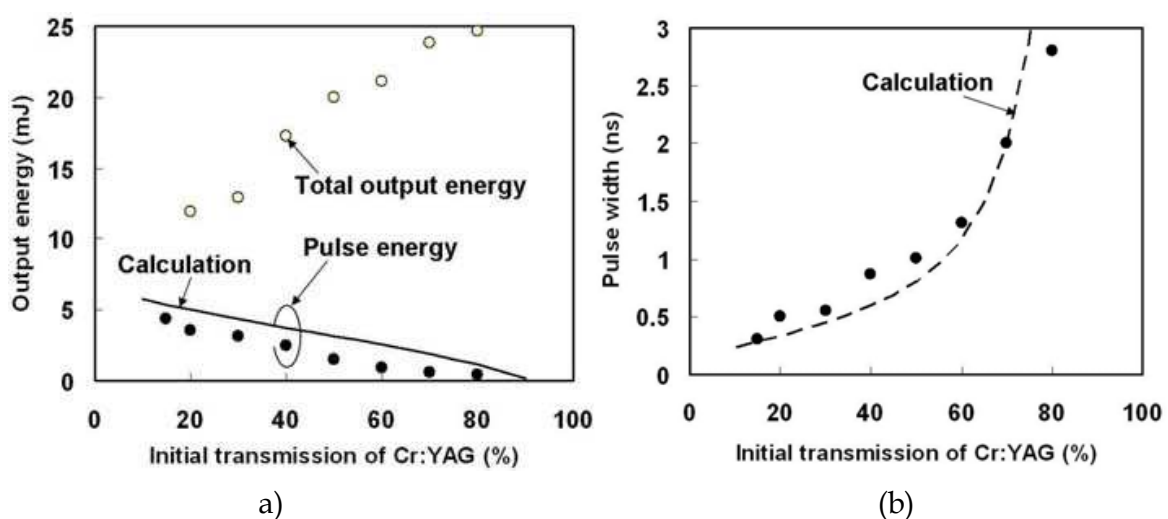


Fig. 3. (a) Output energy and (b) pulse width of the passively Q-switched micro-laser as a function of the initial transmission of Cr:YAG.

In the theoretical calculations shown in Fig.3, we assumed the ground-state absorption cross section of $\text{Cr}^{4+}:\text{YAG}$ as $\sigma_{\text{SA}}=2\times 10^{-18} \text{ cm}^2$ and the excited-state absorption as $\sigma_{\text{ESA}}=5\times 10^{-19} \text{ cm}^2$. These are very important parameters but vary greatly in previous reports hence we used the averaged values in recent reports (Burshtein et al., 1998; Xiao et al., 1999; Feldman et al., 2003). In the calculation of pulse energy, we also assumed that the laser mode has the same size as the pump beam. Theoretically the output pulse energy is proportional to the area of the laser mode, so it is understood that the actual laser mode size is smaller by 10% or more than the pump beam due to the aperture effect of the saturable absorber of a Cr:YAG crystal as shown in Fig.3(a). As the initial transmission is higher, the discrepancy is larger. On the other hand, the calculation of pulse width agrees well with the experimental results as seen in Fig.3 (b), because the calculation of pulse width has no relation to the size of the modes. Though the highest pulse energy and shortest pulse width were obtained at an initial Cr:YAG transmission of 15%, optical damage was observed at the output coupler and then the beam quality was degraded. The beam quality was also degraded at initial transmissions of higher than 70%, because the aperture effect of a Cr:YAG crystal is weak.

To use a laser for ignition, optical intensities of the order of $100\text{GW}/\text{cm}^2$ are necessary at the focal point for breakdown. From our experimental observations, stable breakdown in air was observed at a pulse energy larger than 1.5mJ and a pulse width less than 1ns using an aspheric focus lens with a focal length of 10mm . In addition to the pulse energy, the total output energy is also necessary to ignite fuel-lean mixtures as discussed later. However as seen in Fig.3(a) the pulse energy and the total output energy are in the conflicting relation. Therefore we selected 30% as an optimum initial transmission of a Cr:YAG saturable absorber in our laser configurations. The laser performances were tested in detail and finally it was applied to the combustion experiments in the optimum condition.

Figure 4 shows the laser output energy and optical-to-optical conversion efficiency as a function of pump duration at an initial Cr:YAG transmission of 30%. As a unique characteristic of passively Q-switched lasers, the output pulse energy is constant until the following pulse is generated, then the output characteristic changes to the shape of stairs. The interval of pulse generation is almost constant at $100\mu\text{s}$. The output energy obtained was 2.7mJ per pulse and totally 11.7mJ (sum of 4 pulses) was obtained at a pump duration of $500\mu\text{s}$. The optical-to-optical conversion efficiency changes largely and periodically by the pump duration and the maximum efficiency of 19% was obtained at the durations of pulse generation.

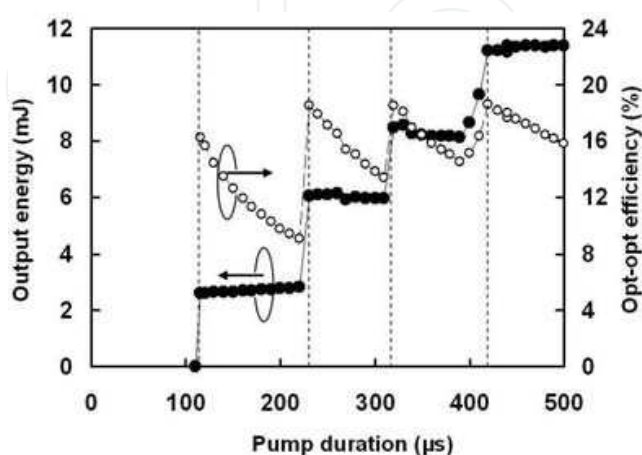


Fig. 4. Output energy and optical-to-optical conversion efficiency as a function of pump duration at an initial transmission of 30%.

Figure 5 shows the fluctuation of the total output energy as a function of pump duration which was estimated statistically from 500 consecutive pulses. The perpendicular dotted lines show the pump durations at which the number of pulses increases as shown in Fig.4. It is understood that the fluctuation increases by increase in the number of pulses and at the duration when the number of pulses changes. The fluctuation is still less than 100μJ (3%).

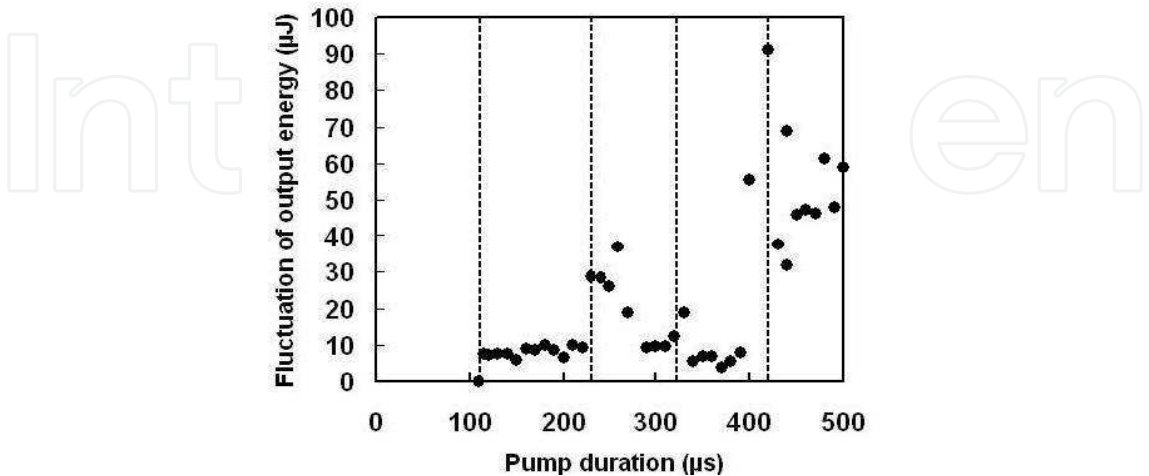


Fig. 5. Fluctuation of the total output energy as a function of pump duration which was estimated statistically from 500 consecutive pulses.

Figure 6 shows (a) the delay times of the each laser pulse from the standup of the pump LD current and (b) the jitters (standard deviation) of the delay times estimated statistically from 500 consecutive pulses as a function of pump duration. As seen in Fig.6 (a), the delay times are not dependent on the pump duration. The pulse interval is constant around 100μs and is equal to the interval of pulse generation. On the other hand, the jitter of the delay time strongly depends on the pump duration and also on the number of pulses. The first pulse has a small jitter for 200ns or less, and it is not dependent on pump duration, but the pulses generated later have a large jitter of 1μs or more, and the jitter changes sharply with the

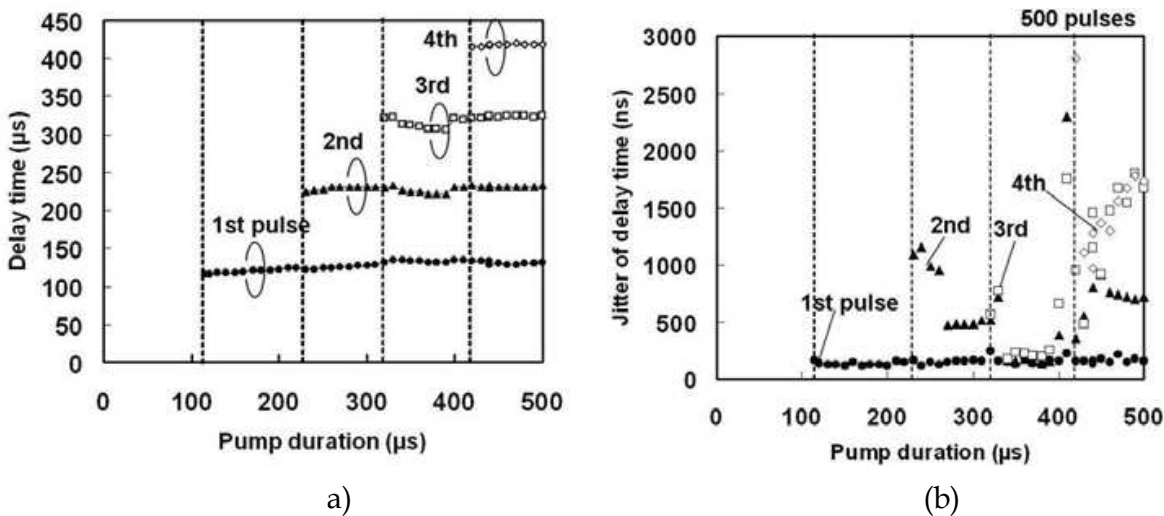


Fig. 6. (a) Delay times of the each laser pulse from the standup of the pump LD current and (b) jitters (standard deviation) of the delay times estimated statistically from 500 consecutive pulses, as a function of pump duration

pump duration as seen in Fig.6 (b). Thermal lens and distortion which grow during QCW excitation in the Nd:YAG crystal strongly influence oscillation timing of a laser pulse. Then the jitter becomes large in the pulse generated later. However it should be mentioned that the jitter of the micro-laser is still 0.5% or less, and are much smaller than CW-pumped passively Q-switched lasers which have pulse-to-pulse jitters of 10% or more. This is because the oscillation condition is thermally initialized by low repetition rate, QCW pumping. It was confirmed that the fluctuation and jitter of the passively Q-switched micro-laser in QCW operations were within the tolerance limits for actual automobile applications.

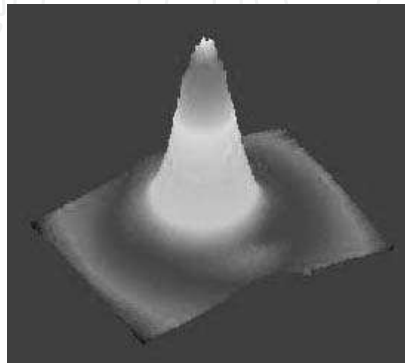


Fig. 7. 3D intensity profile of the output beam (first pulse) at a pump duration of 130 μ s.

Figure 7 shows the 3D intensity profile of the output beam (first pulse) measured by Beam Star-FX33D (Ophir) at a pump duration of 130 μ s. The M^2 value was calculated as 1.2. The beam profile does not change largely by changing the repetition rate from 1 to 100Hz. The pulse width was 600ps as measured in Fig.3(b) the brightness of the micro-laser was calculated as 0.3PW/sr-cm² which is one order of higher than our previous report (Sakai, 2008). To confirm the aperture effect of a Cr:YAG saturable absorber, we measured the beam quality of a micro-laser without the Cr:YAG crystal. The cavity length of 8mm and the output coupler with a reflectivity of 10% were employed to simulate the similar laser mode size in a cavity and threshold (cavity loss) as the passively Q-switched laser. The M^2 value of the simulated laser was measured to be 5 or more. Therefore it is understood that the saturable absorber works effectively as an aperture in the laser cavity. In our optimum designed micro-laser, each pulse of multipulse train has almost the same energy, pulse width and beam quality, hence each pulse can generate breakdown plasma independently in a fuel-mixture.

3.2 High temperature operation of passively Q-switched laser

For the practical use of laser igniters, stable operation is required at temperatures of up to 150°C. Thus, we tested the operation of a passively Q-switched Nd:YAG/Cr:YAG laser at high temperature. First, we studied the temperature dependence of the transmission of a Cr:YAG saturable absorber at a wavelength of 1064nm. Three Cr:YAG crystals with different crystal orientations of <100>, <110> and <111> were prepared. The <100> is popular for passive Q-switching, while the <110> is used for polarization stabilized operation. They have the same initial transmission of 30% at 1064nm and at room temperature. Antireflection (<0.2%) coatings at 1064nm were performed to both surfaces of all the samples. The temperatures of the crystals were controlled by a thermo-electric heater. As incident light sources, we used a commercial CW Nd:YVO₄ laser (MIL-1064-100-5,

Broadband, Inc.) for measurement of the initial transmissions and the passively Q-switched micro-laser we developed for measurement of the saturated transmissions of the Cr:YAG crystals. The polarization of the incident beams to the crystals was linear and rotated by a quarter wave plate in front of the crystals. Figure 8 shows the initial transmissions of the Cr:YAG crystals as a function of crystal temperature. The incident beam had a power of 5mW CW and a diameter of 2mm in the crystals. Slight, 5% increases of initial transmissions were observed with increase in crystal temperatures from 25 to 150°C for all the crystals.

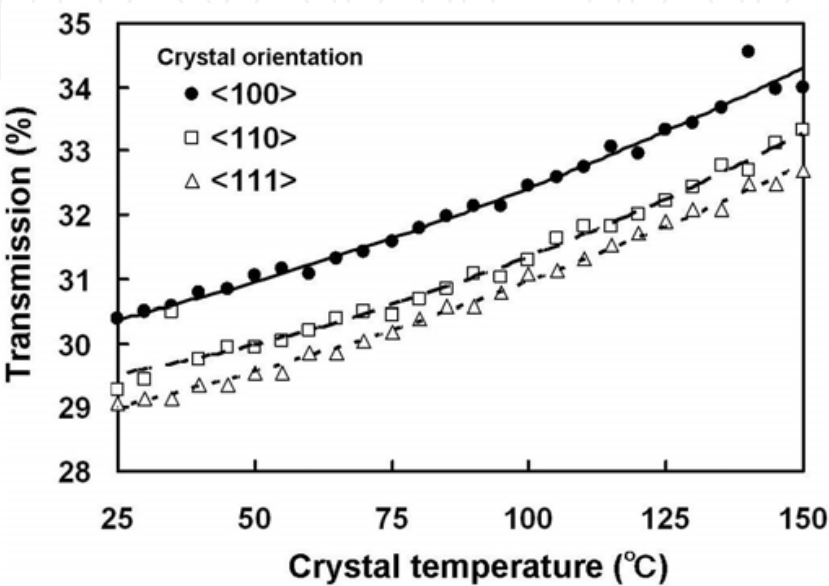


Fig. 8. Initial transmissions of the Cr:YAG crystals with three different orientations as a function of crystal temperature

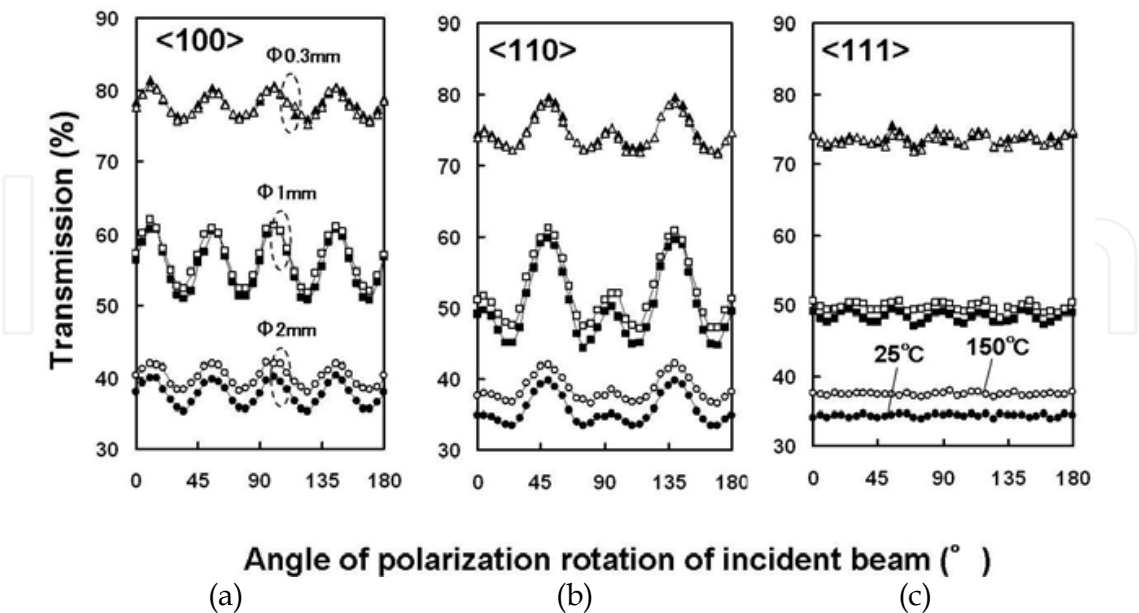


Fig. 9. Saturated transmissions of Cr:YAG crystals at 25°C and 150°C with crystal orientations of (a) <100>, (b) <110>, and (c) <111> as a function of the angle of incident beam polarization rotation.

Figure 9 shows the transition of the saturated transmissions of the Cr:YAG crystals as a function of the angle of incident beam polarization rotation at temperatures of 25 and 150°C and at three different incident beam diameters of 0.3, 1 and 2 mm. The crystal orientations in (a), (b), and (c) are $\langle 100 \rangle$, $\langle 110 \rangle$, and $\langle 111 \rangle$, respectively. The incident Q-switched pulse had an energy of 2mJ constant and a width of 600ps. As seen in these figures, it is understood that the saturated transmissions at the highest beam intensity with a diameter of 0.3mm are the same for both temperatures and the situation is independent on a crystal orientation. Therefore it is expected that the performance of a Cr:YAG saturable absorber dose not change even at 150°C.

Figure 10 (a) shows the input-output characteristics of a Nd:YAG laser without a Cr:YAG crystal at various crystal temperatures of up to 150°C. The temperature-controlled Nd:YAG crystal was longitudinally pumped by a fiber-coupled LD with QCW operation (peak pump power 120W, repetition rate 1Hz). The cavity length was 20mm and the reflectivity of the flat output coupler was reduced to 10% to simulate a cavity loss by a Cr:YAG crystal. As seen in the figure, as the temperature of the Nd:YAG crystal increases from room temperature to 150°C, the threshold increases by 60% and the slope efficiency decreases.

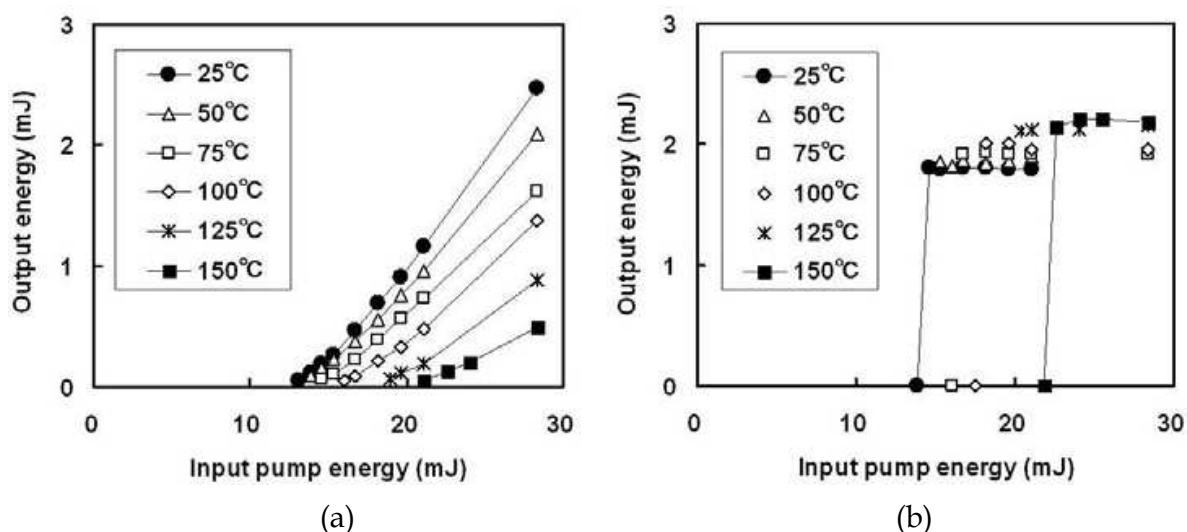


Fig. 10. (a) Input-output characteristics of a Nd:YAG laser without a Cr:YAG crystal at various crystal temperatures of up to 150°C, and (b) input-output characteristics of a Nd:YAG/Cr:YAG passively Q-switched laser at the same crystal temperatures.

Figure 10 (b) shows the input-output characteristics of a Nd:YAG/Cr:YAG passively Q-switched laser at various crystal temperatures. The temperatures of the two crystals are the same, and the pump and cavity layouts are the same as those of the Nd:YAG laser shown in Fig.10 (a), but the reflectivity of the output coupler is 50%. The initial transmission of the Cr:YAG crystal is 30% at room temperature. The experimental data at 20°C and 150°C are connected with a line only so that the results may be understood clearly. The thresholds of the passively Q-switched laser at 20°C and 150°C are almost equivalent to those of the Nd:YAG laser at the same temperatures shown in Fig.10 (a), and we can understand that the characteristics of the Cr:YAG/Nd:YAG passively Q-switched laser at 150°C are mainly decided by that of a Nd:YAG crystal (Tsunekane & Taira, 2009). It should be also emphasized that the output pulse energy increases slightly even as the temperature of the crystals increases to 150°C. From the results, we can further confirm that the Nd:YAG/Cr:YAG passively Q-switched micro-laser is a suitable light source for laser ignition.

4. Ignition in constant volume chamber

The laser ignitions for stoichiometric to fuel-lean C_3H_8 /air mixtures by a high-brightness passively Q-switched micro-laser were studied and compared with a conventional electric spark plug experimentally in a constant-volume ($\sim 200\text{cm}^3$) chamber at room temperature (25°C) and atmospheric pressure (100kPa). The C_3H_8 gas and air were introduced in the combustion chamber after mixing it thoroughly in specified ratios within another chamber beforehand. The ignition experiment was conducted after the flow of the combustible mixture in the chamber settled. The chamber is equipped with three windows. Two of them are laterally opposite to each other for flow visualization and one is for introduction of a laser light or a spark plug (compatible window). The combustion processes were observed by Schlieren photography (shadowgraph) which can visualize a slight refractive-index gradient of transparent media. Highly uniform, incoherent light from a Xenon lamp was introduced to the chamber and the 2D images of the transmitted light through the windows were detected by a high-speed video camera (25000 fps) synchronized with a laser pulse or an electric trigger.

Figure 11 shows the Schlieren photographs of the early stage of ignition and subsequent combustion ignited by (a) a micro-laser and (b) a spark plug in stoichiometric mixture. The air fuel ratio (A/F) is 15.3. The total energy from the laser is $\sim 9\text{mJ}$ (3 pulses) and the input electric energy to the plug is 35mJ . The laser beam is focused inside the chamber through the window by an aspheric lens with a focal length of 10mm so as to have the same ignition position as the spark plug. Then both images show the same position with the same scale in the chamber. The numbers indicate time after a laser shot or an electric trigger on. As shown in the lowermost figures of Fig.11 (a) and (b), the cross-section area of the flame kernel generated by the laser is 3 times larger than the spark plug at 6ms after ignition, even though the ignition energy of the laser is $1/3$ (Tsunekane et al., 2008). Therefore it is confirmed that laser ignition effectively accelerates the flame kernel growth due to the absence of quenching effect by electrodes.

The combustions in the fuel-lean mixtures where the ratio of air increased were observed using the same constant-volume chamber. The A/Fs of the mixtures were changed from 15.2 (stoichiometric) to 18.1. The numbers of laser pulses (pulse train) were also changed

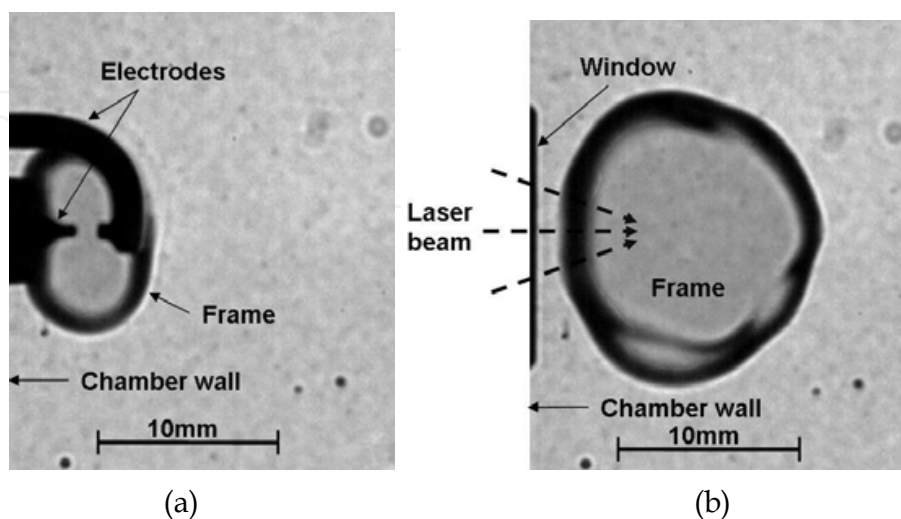


Fig. 11. Schlieren photographs for early stage of ignition in a constant-volume chamber ignited by (a) a micro-laser and (b) a spark plug in a stoichiometric mixture.

		Ignition probability (%)					Spark Plug
		Laser					
C ₃ H ₈ +Air		1 pulse (3.0mJ)	2 pulses (5.6mJ)	3 pulses (8.1mJ)	4 pulses (10.6mJ)	5 pulses (13.0mJ)	
ER	A/F						
1.00	15.2	100	100	100	100	100	100
0.97	15.7	0	50	100	100	100	33
0.93	16.3	–	0	100	60	100	0
0.88	17.2	–	–	22	0	100	–
0.84	18.1	–	–	–	0	0	–

Table 1. Ignition probabilities for complete combustion in a stoichiometric and fuel-lean mixtures in a constant-volume chamber estimated from the repetitive ignition.

from 1 to 5 by changing the pump duration to understand the effect of the total optical energy on combustion. Table 1 summarizes the ignition probabilities for complete combustion estimated from the repetitive ignition experiments in each condition. The horizontal lines show the numbers of laser pulses and the total optical energies, and the right end shows the experimental results from a spark plug. The vertical lines show the A/Fs. The values become high toward the bottom which means the mixtures become leaner. ER is equivalent ratio, the value that broke the A/F (15.2) of the stoichiometric mixture by the A/F of the specific mixture. From this table, it can be seen that the ignition probability of a leaner mixture improves with increase in the number of laser pulses. Then it is understood that higher total ignition energy is necessary for a leaner mixture. One hundred percent ignition is accomplished in the fuel-lean mixture of A/F of 17.2 by 5 laser pulses (5-pulse train) with the total optical energy of 13mJ. Such a multiple pulse ignition is advantageous for actual applications compared to conventional laser ignition by a single big pulse with an optical energy of more than 10mJ. The peak intensity of a laser pulse can be reduced by maintaining total ignition energy, and the optical damage to coatings on optics can be avoided. Moreover, the number of pump LDs can be reduced. It has the advantage not only of miniaturization of the ignition system but also of low price.

From these experimental results of laser ignition by a micro-laser, it should be mentioned that in a stoichiometric mixture, 100% ignition was accomplished by a single pulse with an optical energy of 3mJ. From the Schlieren photography measurements, it was observed that in the lean mixtures, the first laser pulse (3mJ) was still enough for breakdown and flame kernel formation, but the growth of the flamee kernel was slow compared to that in the stoichiometric mixture and disappeared quickly if the following pulses were not injected.

In the case of spark plug ignition shown in the right end, the ignition probability is below 100% even in an A/F of 15.7, which is slightly leaner than in a stoichiometric mixture. Schlieren photography also demonstrated that the growth of the flamee kernel was slow and the time during the boundary of the flame kernel in contact with the electrodes was long, and therefore it could be understood that the quenching effect by electrodes of a spark plug was more significant in lean mixtures.

5. Ignition in real automobile engine

Finally, ignition tests for a real automobile engine were performed. We used a commercial engine of 1AZ-FSE (TOYOTA Motor Corp.), which is a 2.0 L, straight-4 piston engine with a gasoline direct injection system. Figure 12 shows the optical layout for laser ignition. The micro-laser module was fixed not on the engine directly but on a metal frame closely positioned on the upper side of the engine and the output beam was carefully aligned by using three mirrors to the optical axis of the focal lens fixed in the spark plug hole. The optical path from the module to the focal lens was around 830mm. A transmission lens with a focal length of 300mm was used to control the beam size. The focal lens had a focal length of 10mm. The ignition point of a laser was set to be the same point as a spark plug by tuning the height of the focal lens. Thus this experiment was not optimized for laser ignition. In this experiment, three of the four cylinders (from #1 to #3) were ignited by conventional spark plugs and the #4 cylinder was ignited by a laser. Each ignition timing was carefully controlled and optimized. The repletion rates of the igniters were 13.3Hz corresponding to an engine speed of 1600rpm.

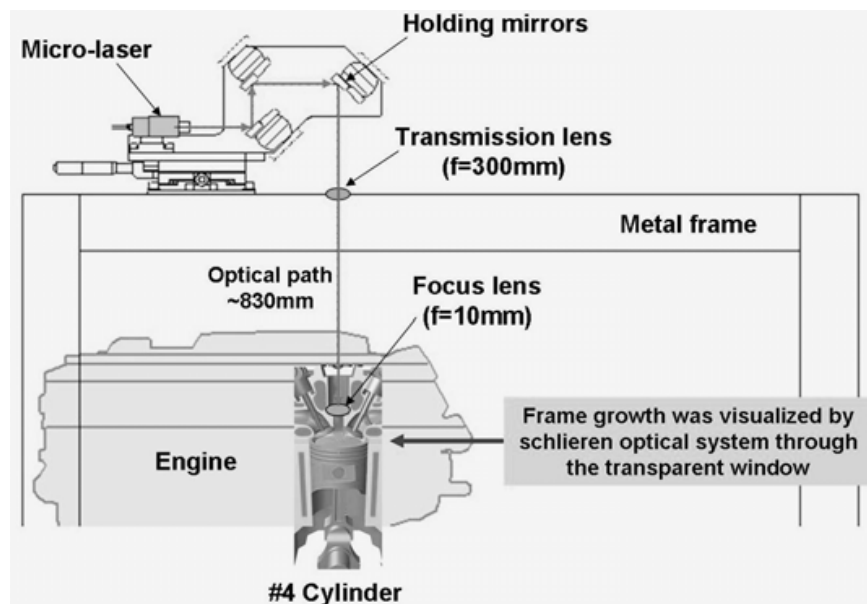


Fig. 12. Optical layout of laser ignition experiments for a real engine

The experimental setup for visualization of combustion with reflective Schlieren photography is schematically shown in Fig.13. The collimated and highly homogenized light from a Xenon lamp was introduced into the combustion chamber through a transparent window which was formed at the side wall of the cylinder head of #4 and was reflected back at a mirror, which was situated inside the cylinder wall at the opposite side of the window. The reflected light was imaged by a high-speed CCD camera (25000fps). Laser beam was introduced into the chamber through a normal spark plug hole.

Schlieren photographs of the early stage of ignition and subsequent combustion in a real engine are summarized in Fig.14. In the micro-laser ignitions, combustion processed images of three different pulse-trains, i.e., single-pulse, two-pulse and four-pulse trains, are demonstrated. The right side shows the image of a conventional spark plug ignition. Total optical energies into the chamber are also shown in brackets, but the energy from the micro-laser decreases to 85% due to optical loss at the three alignment mirrors. In this figure, the

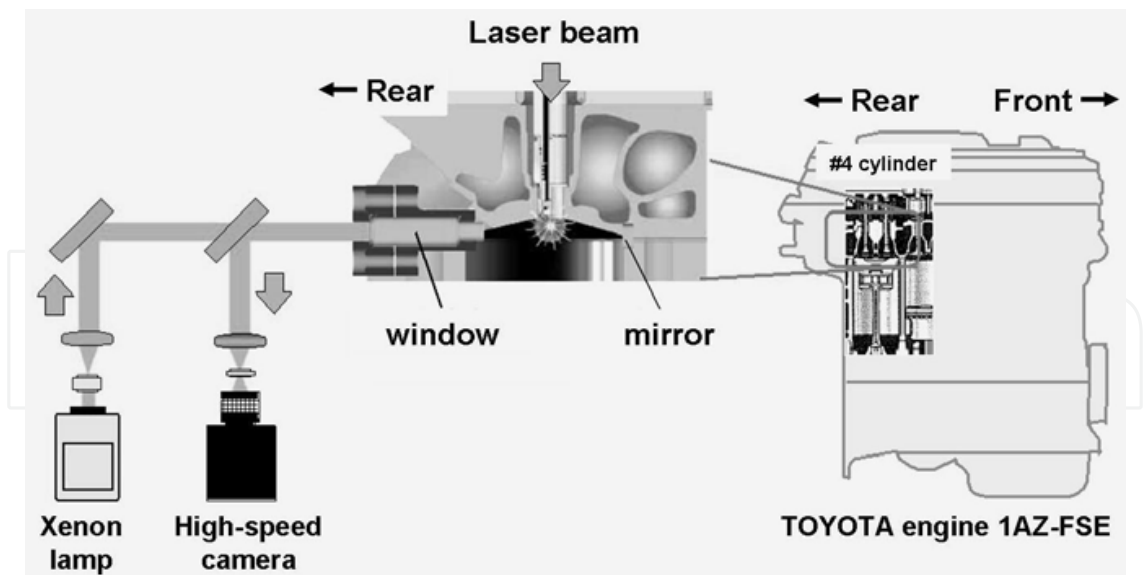


Fig. 13. Experimental setup for visualization of combustion with reflective Schlieren photography

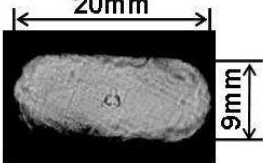
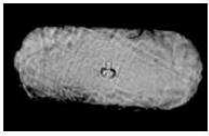
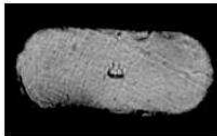
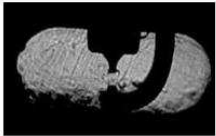
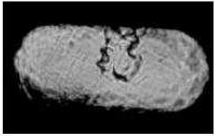
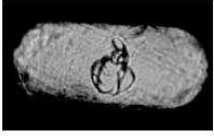
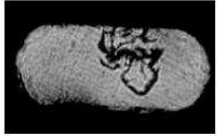

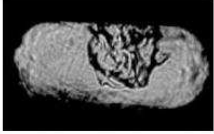

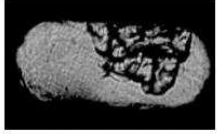
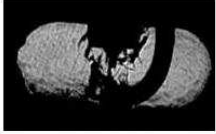
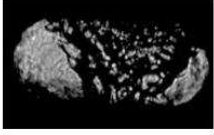
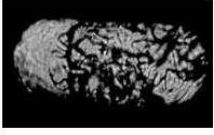
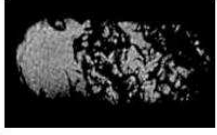

Time from ignition	Micro-laser			Spark plug (35mJ)
	Single pulse (2.3mJ)	Two-pulse train (5.0mJ)	Four-pulse train (10.4mJ)	
40μs				
600μs				
1000μs				
1800μs				

Fig. 14. Schlieren photographs of the early stage of ignitions by a micro-laser and a spark plug and the subsequent combustions in a real engine

A/F is 14.5, which is a stoichiometric mixture of gasoline and air. It should be emphasized that a single laser pulse with an energy of 2.3mJ can successfully ignite a real engine. We think this will be the lowest energy ever reported for laser ignition of a real automobile

engine. High-brightness, passively Q-switched micro-laser can reduce the ignition energy dramatically compared with previous ignition lasers (Kroupa, 2009) and a spark plug. The operation of an engine ignited by a single laser pulse is quite stable and no miss-ignitions appeared during our experiment for several tens of minutes. However, look carefully at the Schlieren photographs in Fig.14 at the early stage until $1000\mu\text{s}$, and you will find that the shadows of the flames by single and two-pulse trains are weak compared with those of four-pulse train. We think flame growth is perturbed by the flow in the chamber due to lack of total ignition energy. On the other hand, such flow helps a spark plug escape from quenching effect by the electrodes and then the flame grows effectively with a high ignition energy of 35mJ, in contrast with previous experimental results in a static constant-volume chamber.

We also tested in lean mixtures. The lean limit (A/F), where the combustion was slightly unstable, of single-pulse, two-pulse and four-pulse were 16, 17.6, and 18.8, respectively, but a spark plug had a higher lean limit of 20~21. We think the total optical energy of a laser needs up to 20mJ, where the lean limit of laser ignition will be comparable with that of spark plug ignition. Recently the maximum total output energy of 21mJ was obtained with an optical-to-optical conversion efficiency of 23% from the same micro-laser module by increasing of the peak power of fiber-coupled pump diode to 180W.

From the Schlieren photography, it is understood that the flame-growing processes of laser and electric spark plug ignitions at the early stage are quite different. In a spark plug, the flame generated at the gap of the electrodes forms an eddy structure and stays around the outer electrode, and grows continuously and stably to a large flame. On the other hand, the flame generated by a laser moves randomly in the free space of the chamber by turbulent flow during the growth.

The contamination and damage of an optical window in the combustion chamber are well-known serious problems of laser ignition (Ranner et al., 2007). In our experiments, Al_2O_3 was used as a window material. No visual contaminations and no damages were observed on the window surface after the combustion experiments for several hours, but long-duration tests under various engine conditions are necessary for choice and optimization of practical windows.

6. Real spark plug size micro-laser module

In Fig.15, we show the first prototype micro-laser module which has the same dimensions as a spark plug. This module includes not only pumping optics from a fiber to a solid-state material but also beam expanding and focusing optics for ignition. The laser igniter has the same optical design and the same performance as the experimental module in Fig.2, and it is physically possible to ignite a real engine by installing it instead of a spark plug to a plug hole. For real operation on an engine, however, the mechanical design inside the module should be improved to sustain the high temperature (up to 150°C) and vibration of a real engine. In this report, we used conventional single crystals, but we think YAG ceramics are promising actual light sources for laser ignition, because they have higher uniformity and stress resistance, and are suitable for mass-production. In addition, if a composite structure of Nd:YAG/Cr:YAG is possible, then the compact and rugged, monolithic laser cavity will be made (Feng, 2004; Taira, 2007).



Fig. 15. Prototype spark plug size micro-laser head and a conventional spark plug

7. Conclusion

A high-brightness, passively Q-switched Nd:YAG/Cr:YAG micro-laser was developed and optimized for ignition of engines. The output energies of 2.7mJ per pulse and 11.7mJ in total (four-pulse train) were obtained at a pump duration of 500μs with an optical-to-optical conversion efficiency of 19%. A pulse duration of 600ps and an M^2 value of 1.2 were obtained and the brightness of the micro-laser was calculated as 0.3PW/sr-cm². The optical power intensity at the focal point of ignition was calculated as 5TW/cm². The fluctuations of the total output energies and jitters of the delay time of a laser oscillation were less than 100μJ (3%) and 0.5%, respectively. We further confirmed that the output pulse energy of a passively Q-switched Nd:YAG/Cr:YAG laser did not change even though the temperature of the crystals increases to 150°C. The enhanced combustion by the micro-laser ignition was successfully demonstrated in a constant-volume chamber with room temperature and with atmospheric pressure. The cross-section area of a flame kernel generated by the micro-laser was 3 times larger than a spark plug at 6ms after ignition in a stoichiometric mixture (A/F 15.2) of C₃H₈/air. The effective laser ignition for lean mixtures was also accomplished by a multiple pulse (pulse train) of the micro-laser. Ignition of 100% was successfully demonstrated by a five-pulse train in a lean mixture of an A/F 17.2, where spark plug ignition failed. Finally, ignition tests for a real automobile engine were performed. A single laser pulse with an energy of 2.3mJ could ignite and drive the engine stably. It will be lowest energy ever reported for laser ignition of a real automobile engine. We can confirm that an optimally designed, high-brightness, passively Q-switched micro-laser reduced the ignition energy dramatically compared with previous ignition lasers and a spark plug and the dimension of the laser head can be reduced to real spark plug size.

8. Acknowledgment

We are grateful to Japan Science and Technology Agency (JST) for financial support on Practical Application Research of “Micro solid-state laser for internal-combustion engine

control" promoted by JST Innovation Plaza Tokai (2006-2009). We thank Dr. Fujikawa of Toyota Central R&D Labs., Inc. for technical discussion of combustion and Mr. Mizutani of the equipment development division of IMS for fabrication of the micro-laser modules.

9. References

- Hickling, R. & Smith, W. R. (1974). Combustion bomb tests of laser ignition, SAE Paper no.740114
- Dale, J. D.; Checkel, M. D. & Smy, P. R. (1997). Application of high energy ignition systems to engines, *Prog. Energy Combust. Sci.* vol.23, pp379-398
- Phuoc, T. X. (2006). Laser-induced spark ignition fundamental and applications, *Opt. Lasers Eng.* vol.44, pp351-397
- Phuoc, T. X. (2000). Single-point versus multi-point laser ignition: experimental measurements of combustion times and pressures, *Combustion and Flame* vol.122, pp.508-512
- Morsy, M. H. ; Ko, Y. S., Chung, S. H. & Cho, P. (2001). Laser-induced two-point ignition of premixture with a single-shot laser, *Combustion and Flame* vol.125, pp724-727
- Weinrotter, M.; Kopecek, H., Tesch, M., Wintner, E., Lackner, M. & Winter, F. (2005). Laser ignition of ultra-lean methane/hydrogen/air mixtures at high temperature and pressure, *Exp. Thermal and Fluid Sci.*, vol.29, pp.569-577
- Joshi, S.; Yalin, A. P. & Galvanauskas, A. (2007). Use of hollow core fibers, fiber lasers, and photonic crystal fibers for spark delivery and laser ignition in gases, *Appl. Opt.*, vol.46, pp.4057-4064
- Kofler, H.; Tauer, J., Tartar, G., Iskra, K., Klausner, J., Herdin, G. & Wintner, E. (2007). An innovative solid-state laser for engine ignition, *Laser Phys. Lett.* vol.4, pp322-327
- Zaykowski, J. J. & Dill III, C. (1994). Diode-pumped passively Q-switched picosecond microchip lasers, *Opt. Lett.* vol.19, pp.1427-1429
- Sakai, H.; Kan, H. & Taira, T. (2008). >1MW peak power single-mode high-brightness passively Q-switched Nd³⁺:YAG microchip laser, *Opt. Exp.* vol.16, pp.19891-19899
- Huang, S-L.; Tsui, T-Y., Wang, C-H. & Kao, F-J. (1999). Timing jitter reduction of a passively Q-switched laser, *Jpn. J. Appl. Phys.* vol.38, pp.L239-241
- Tang, D. Y.; Ng, S. P., Qin, L. J. & Meng, X. L. (2003). Deterministic chaos in a diode-pumped Nd:YAG laser passively Q switched by a Cr⁴⁺:YAG crystal, *Opt. Lett.*, vol.28, pp.325-327
- Szabo, A. & Stein, R. A. (1965). Theory of laser giant pulsing by a saturable absorber, *J. Appl. Phys.* vol.36, 1562-1566
- Degnan, J.J. (1995). Optimization of passively Q-switched lasers, *IEEE J. Quantum Electron.*, vol.31, pp.1890-1901, Nov.
- Xiao, G. & Bass, M. (1997). A generalized model for passively Q-switched lasers including excited state absorption in the saturable absorber, *IEEE J. Quantum Electron.*, vol.33, pp.41-44, Jan.
- Zhang, X.; Zhao, S., Wang, Q., Zhang, Q., Sun, L. & Zhang, S. (1997). Optimization of Cr⁴⁺-doped saturable-absorber Q-switched lasers, *IEEE J. Quantum Electron.*, vol.33, pp.2286-2294

- Chen, Y. F.; Lan, Y. P. & Chang, H. L. (2001). Analytical model for design criteria of passively Q-switched lasers, *IEEE J. Quantum Electron.*, vol.37, pp.462-468, March
- Pavel, N.; Saikawa, J., Kurimura, S. & Taira, T. (2001). High average power diode end-pumped composite Nd:YAG laser passively Q-switched by Cr:YAG saturable absorber, *Jpn. J. Appl. Phys.* vol.40, pp.1253-1259, March
- Patel, F. D. & Beach, R. J. (2001). New formalism for the analysis of passively Q-switched laser systems, *IEEE J. Quantum Electron.*, vol.37, pp.707-715, May
- Zabkar, J.; Marincek, M. & Zgonik, M. (2008). Mode competition during the pulse formation in passively Q-switched Nd:YAG lasers, *IEEE J. Quantum Electron.*, vol.44, pp.312-318, Apr.
- Tsunekane, M.; Inohara, T., Ando, A., Kanehara, K. & Taira, T. (2008). High peak power, passively Q-switched Cr:YAG/Nd:YAG micro-laser for ignition of engines, in *Proc. Advanced Solid State Photonics*, OSA Tech. Dig., MB4, Jan.
- Zaykowski, J. J. & Wilson Jr., A. L. (2003). Pump-induced bleaching of the saturable absorber in short-pulse Nd:YAG/Cr⁴⁺:YAG passively Q-switched microchip lasers, *IEEE J. Quantum Electron.*, vol.39, pp.1588-1593, Dec.
- Jaspan, M. A.; Welford, D. & Russell, J. A. (2004). Passively Q-switched microlaser performance in the presence of pump induced bleaching of the saturable absorber, *Appl. Opt.*, vol.43, pp.2555-2560, Apr.
- Burshtein, Z.; Blau, P., Kalisky, Y., Shimony, Y. & Kokta, M. R. (1998). Excited-state absorption studies of Cr⁴⁺ ions in several garnet host crystals, *IEEE J. Quantum Electron.*, vol.34, pp.292-299, Feb.
- Xiao, G.; Lim, J. H., Yang, S., Stryland, E. V., Bass, M. & Weichman, L. (1999). Z-scan measurement of the ground and excited state absorption cross sections of Cr⁴⁺ in yttrium aluminum garnet, *IEEE J. Quantum Electron.*, vol.35, pp.1086-1091, July
- Feldman, R.; Shimony, Y. & Burshtein, Z. (2003). Dynamics of chromium ion valence transformations in Cr,Ca:YAG crystals used as laser gain and passive Q-switching media, *Opt. Mat.*, vol.24, pp.333-344
- Tsunekane, M.; Inohara, T., Ando, A., Kanehara, K. & Taira, T. (2008). Compact, high peak power, passively Q-switched micro-laser for ignition of engines, in *Proc. Conf. Laser Electro-Optics.*, OSA Tech. Dig. CFJ4
- Tsunekane, M.; Inohara, T., Ando, A., Kanehara, K. & Taira, T. (2008). Compact and High-brightness Passively Q-switched Cr:YAG/Nd:YAG Laser for Ignition of Engines, in *3rd EPS-QEOD Europhoton conf. Tech. Dig. FROB.2*, Sep.
- Feldman, R.; Shimony, Y. & Burshtein, Z. (2003). Passive Q-switching in Nd:YAG/Cr:YAG monolithic microchip laser, *Opt. Mat.*, vol.24, pp.393-399
- Graham-Rowe, D. (2008). Lasers for engine ignition, *nature photonics* vol.2, pp.515-518, Sep.
- Feng, F.; Lu, J., Takaichi, K., Ueda, K., Yagi, H., Yanagitani, T. & Kaminskii, A. A. (2004). Passively Q-switched ceramic Nd³⁺:YAG/Cr⁴⁺:YAG lasers, *Appl. Opt.*, vol.43, pp.2944-2947, May
- Taira, T. (2007). RE³⁺-ion-doped YAG ceramic lasers (invited), *IEEE J. Sel. Top. Quantum Electron.*, vol.13, pp.798-809, May

- Kroupa, G.; Franz, G. & Winkelhofer, E. (2009). Novel miniaturized high-energy Nd-YAG laser for spark ignition in internal combustion engines, *Opt. Eng.* vol.48, no.1, pp.014202-1 to 5, Jan.
- Tsunekane, M. & Taira, T. (2009). High temperature operation of passively Q-switched, Cr:YAG/Nd:YAG micro-laser for ignition of engines, in *Proc. Conf. Laser Electro-Optics/Europe-EQEC.*, Tech. Dig. CA.P.30, June
- Ranner, H.; Tewari, P. K., Kofler, H., Lackner, M., Wintner, E., Agarwal, A. K. & Winter, F. (2007). Laser cleaning of optical windows in internal combustion engines, *Opt. Eng.* vol.46, no.10, pp.104301-1 to 8, Oct.



Advances in Solid State Lasers Development and Applications

Edited by Mikhail Grishin

ISBN 978-953-7619-80-0

Hard cover, 630 pages

Publisher InTech

Published online 01, February, 2010

Published in print edition February, 2010

Invention of the solid-state laser has initiated the beginning of the laser era. Performance of solid-state lasers improved amazingly during five decades. Nowadays, solid-state lasers remain one of the most rapidly developing branches of laser science and become an increasingly important tool for modern technology. This book represents a selection of chapters exhibiting various investigation directions in the field of solid-state lasers and the cutting edge of related applications. The materials are contributed by leading researchers and each chapter represents a comprehensive study reflecting advances in modern laser physics. Considered topics are intended to meet the needs of both specialists in laser system design and those who use laser techniques in fundamental science and applied research. This book is the result of efforts of experts from different countries. I would like to acknowledge the authors for their contribution to the book. I also wish to acknowledge Vedran Kordic for indispensable technical assistance in the book preparation and publishing.

How to reference

In order to correctly reference this scholarly work, feel free to copy and paste the following:

Masaki Tsunekane, Takayuki Inohara, Kenji Kanehara and Takunori Taira (2010). Micro-Solid-State Laser for Ignition of Automobile Engines, *Advances in Solid State Lasers Development and Applications*, Mikhail Grishin (Ed.), ISBN: 978-953-7619-80-0, InTech, Available from: <http://www.intechopen.com/books/advances-in-solid-state-lasers-development-and-applications/micro-solid-state-laser-for-ignition-of-automobile-engines>

INTECH
open science | open minds

InTech Europe

University Campus STeP Ri
Slavka Krautzeka 83/A
51000 Rijeka, Croatia
Phone: +385 (51) 770 447
Fax: +385 (51) 686 166
www.intechopen.com

InTech China

Unit 405, Office Block, Hotel Equatorial Shanghai
No.65, Yan An Road (West), Shanghai, 200040, China
中国上海市延安西路65号上海国际贵都大饭店办公楼405单元
Phone: +86-21-62489820
Fax: +86-21-62489821

© 2010 The Author(s). Licensee IntechOpen. This chapter is distributed under the terms of the [Creative Commons Attribution-NonCommercial-ShareAlike-3.0 License](https://creativecommons.org/licenses/by-nc-sa/3.0/), which permits use, distribution and reproduction for non-commercial purposes, provided the original is properly cited and derivative works building on this content are distributed under the same license.

IntechOpen

IntechOpen